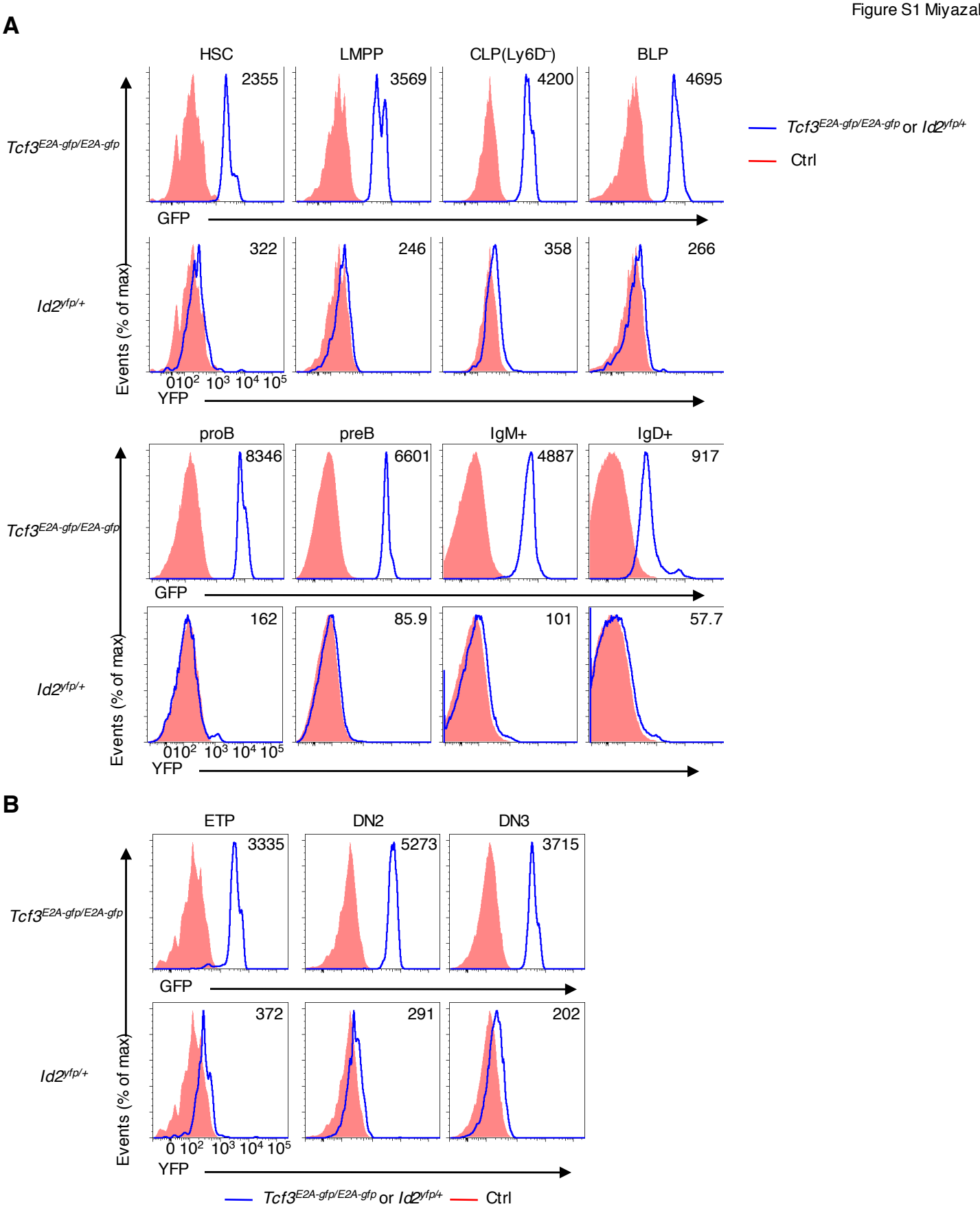

Figure S1 The expression of E2A or Id2 during B cell and T cell development (Related to Figure 1). (**A**),(**B**) Flow cytometric analysis of the expression of GFP (*Tcf3*$^{E2A\text{-}gfp/E2A\text{-}gfp}$) or YFP (*Id2*$^{yfp/+}$). HSC (Lin$^-Kit^+$Sca1$^+$CD150$^+$Flt3$^-$), LMPP (Lin$^-Kit^+$Sca1$^+$Flt3$^-$IL-7R$^-$), CLP (Lin$^-$Flt3$^+$IL-7R$^+$Kit^{mid}Sca1^{mid}Ly6D$^-$), BLP (Lin$^-$Flt3$^+$IL-7R$^+$Kit^{mid}Sca1^{mid}Ly6D$^+$), proB (CD19$^+$B220$^+IgD^-IgM^-Kit^+$CD25$^-$), preB (CD19$^+$B220$^+IgD^-IgM^-Kit^-$CD25$^+$), IgM+ (CD19$^+$B220$^+IgD^-IgM^+$), IgD+ (CD19$^+$B220$^+IgD^+$), ETP (Lin$^-$CD25$^-$CD44$^+Kit^+$), DN2 (Lin$^-$CD25$^+$CD44$^+$), DN3 (Lin$^-$CD25$^+$CD44$^-$). Numbers in plots indicate mean fluorescence intensity (MFI) of GFP and YFP. Two independent experiments produced with similar results.

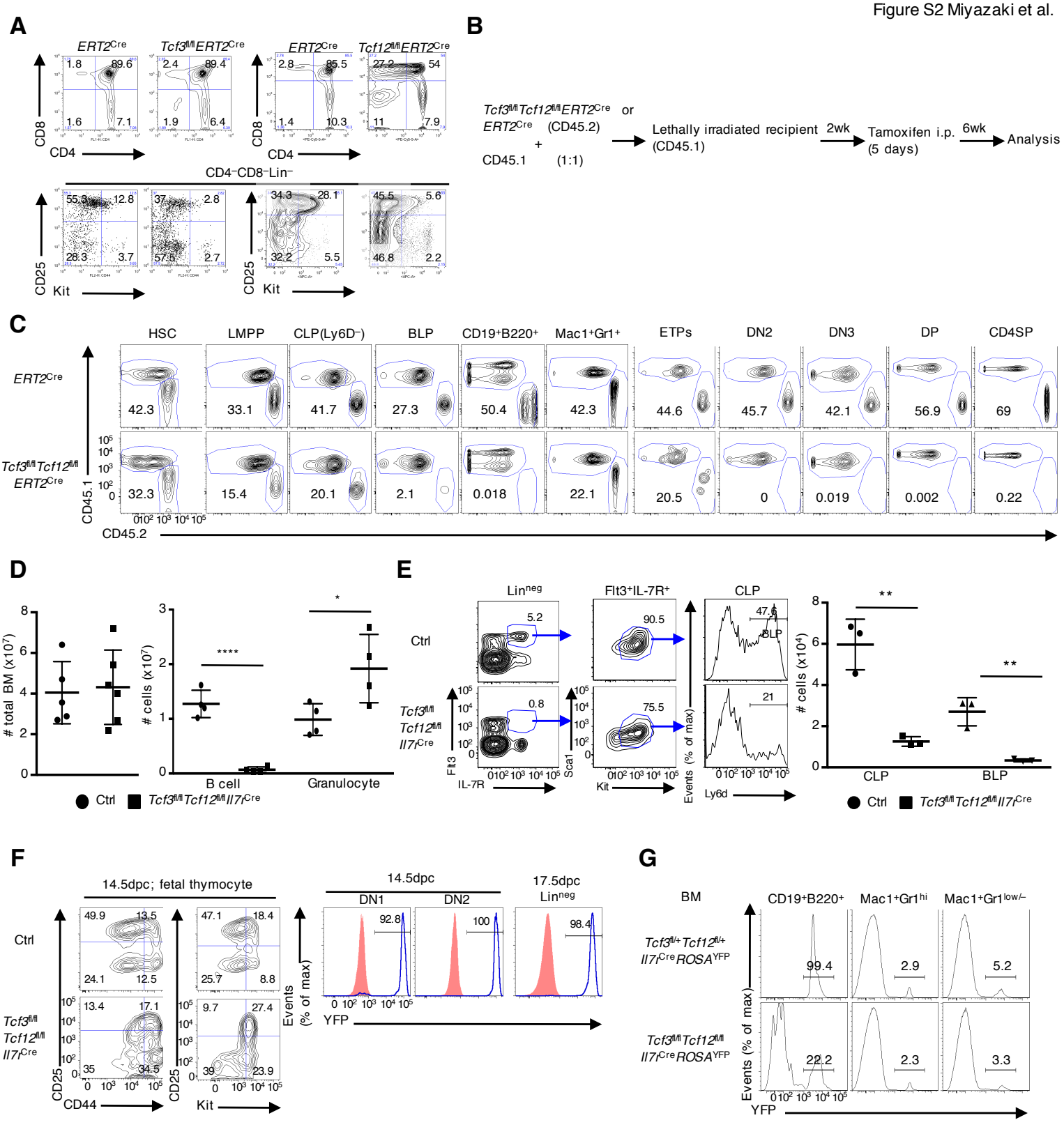

Figure S2 E2A and HEB are crucially required for B cell and T cell development (Related to Figure 2).
(**A**) Flow cytometric analysis of CD4 versus CD8 expression, and Kit versus CD25 expression gated on CD4$^-$CD8$^-$Lin$^-$ thymocytes from *Tcf3*$^{fl/fl}$*ER*^{Cre}, *Tcf12*$^{fl/fl}$*ER*^{Cre}, or *ER*^{Cre} mouse. Numbers in quadrants indicate percent cells in each compartment. (representative from two independent experiments) (**B**) Strategy for competitive bone marrow transplantation using cells derived from *Tcf3*$^{fl/fl}$*Tcf12*$^{fl/fl}$*ERT2*^{Cre} or *ERT2*^{Cre} mice. BM cells were co-transferred with CD45.1 BM cells (1:1 ratio) into lethally irradiated CD45.1 recipient mice. (**C**) Flow cytometric analysis of CD45.1 and CD45.2 expression gated on various stages of bone marrow cells and thymocytes. Numbers in plots indicate the percentage of CD45.2$^+$ cells. See also Figure 2A. (**D**) Cell number of bone marrow cells (left), B cell (CD19$^+$B220$^+$), and Granulocyte (Mac1$^+$Gr1^{hi}) from *Tcf3*$^{fl/fl}$*Tcf12*$^{fl/fl}$*Il7r*^{Cre} or control mice. (n=4, from three independent experiments) (**E**) Gating strategy for CLP and BLP in BM from 4-week-old *Tcf3*$^{fl/fl}$*Tcf12*$^{fl/fl}$*Il7r*^{Cre} or control mouse (left). Numbers in plots indicate percent of cells in outlined areas. Cell number of CLP and BLP in the bone marrow derived from 4-week-old *Tcf3*$^{fl/fl}$*Tcf12*$^{fl/fl}$*Il7r*^{Cre} or control mouse (right). (n=3, from three independent experiments) (**F**) Representative flow cytometric of CD44 versus CD25 (left) and Kit versus CD25 (middle) expression on total thymocytes from 14.5 dpc *Tcf3*$^{fl/fl}$*Tcf12*$^{fl/fl}$*Il7r*^{Cre} or control fetus. The expression of YFP gated on DN1 and DN2 from 14.5 dpc *Tcf3*$^{fl/fl}$*Tcf12*$^{fl/fl}$*Rosa*$^{yfp/yfp}$*Il7r*^{Cre} fetus, and YFP expression gated on Lin$^-$ thymocyte from 17.5 dpc *Tcf3*$^{fl/fl}$*Tcf12*$^{fl/fl}$*Rosa*$^{yfp/yfp}$*Il7r*^{Cre} fetus. (Representative data from two independent littermates (n=9))(**G**) YFP-expression gated on CD19$^+$B220$^+$, Mac1$^+$Gr1^{hi}, and Mac1$^+$Gr1$^{lo/-}$ cells in BM, as seen in Figure 2H. Data represent the mean ± SD. *, $P<0.05$, **, $P<0.01$, ****, $P<0.0001$ (Student's *t* test).

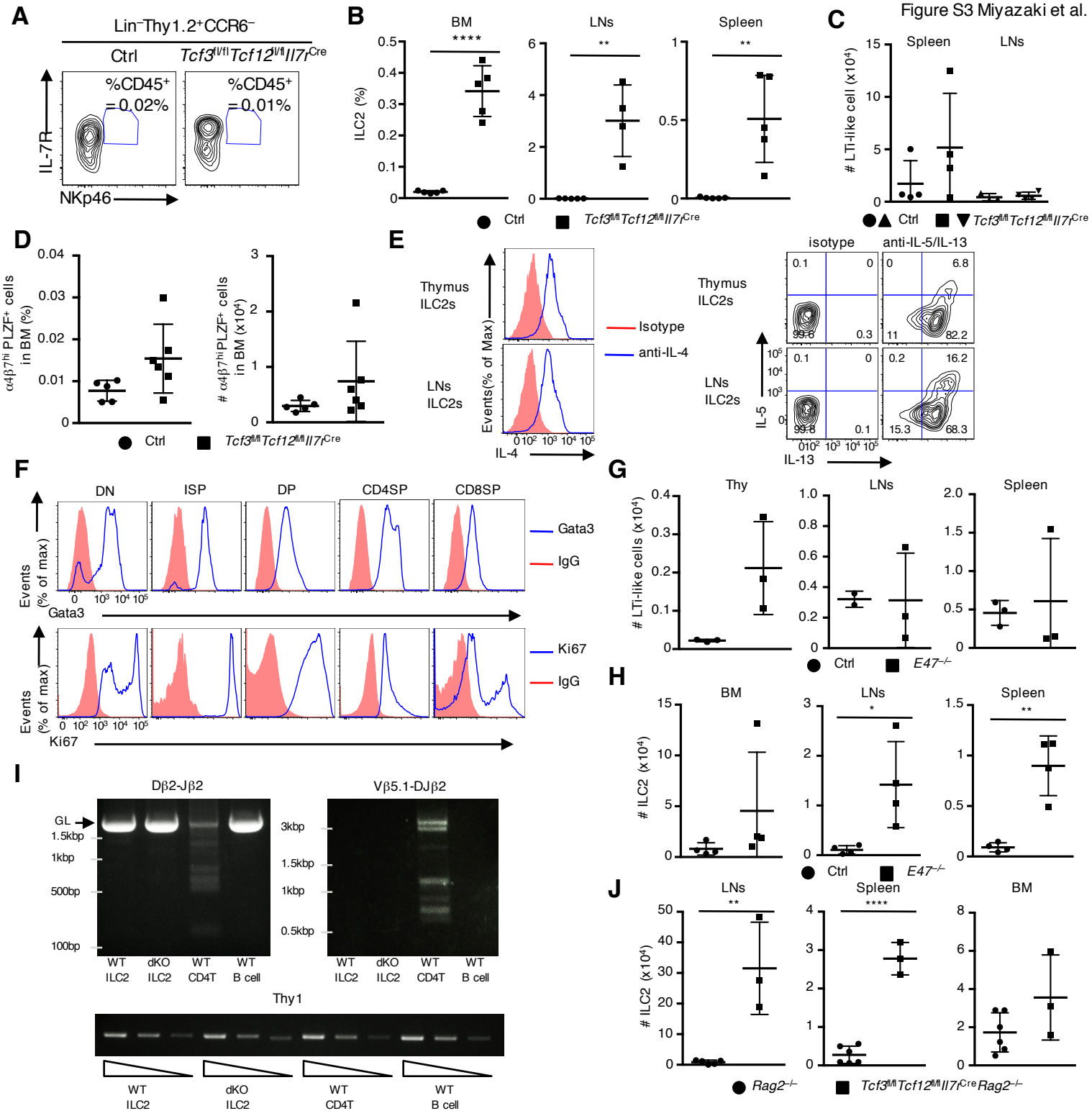

Figure S3 E2A and HEB act in concert to suppress aberrant development of ILCs (Related to Figure 4). (**A**) Flow cytometric analysis of NKp46 versus IL-7R expression gated on Lin⁻Thy1.2⁺CCR6⁻ thymocytes from 4-week-old *Tcf3*$^{fl/fl}$*Tcf12*$^{fl/fl}$*Il7r*^{Cre} or control mouse, as seen in Figure 4. (**B**) Frequency of ILC2 in BM, LNs, and spleen from 4-week-old *Tcf3*$^{fl/fl}$*Tcf12*$^{fl/fl}$*Il7r*^{Cre} or control mouse, as seen in Fig. 5. (n=4-5, from 4 independent experiments) (**C**) Cell number of LTi-like cells in Spleen and LNs, as seen in Fig. 5. (n=4, from three independent experiments) (**D**) Frequency and cell numbers of α4β7^{hi}PLZF⁺ ILC precursor in 4-week-old *Tcf3*$^{fl/fl}$*Tcf12*$^{fl/fl}$*Il7r*^{Cre} or control bone marrow. (n=5-6, from 5 independent experiments) (**E**) Cytokine expression in thymic (top raw) and LNs (bottom) ILC2s derived from *Tcf3*$^{fl/fl}$*Tcf12*$^{fl/fl}$*Il7r*^{Cre} mice. Histogram shows IL-4 expression (red; isotype control, blue; anti-IL-4 antibody). Middle and left panels shows isotype control and anti-IL5/IL-13 antibodies. Sorted ILC2s were cultured in the presence of PMA plus ionomycin in medium containing IL-7. Numbers in quadrants indicate percent cells in each compartment. Data are representative of two independent experiments. (**F**) Flow cytometric analysis of Gata3 (top) and Ki67 (bottom) expression gated on DN, ISP, DP, CD4SP and CD8SP thymocytes from wild-type mouse, as seen in Figure 4B and 4D. One experiment. (**G**) Cell numbers of LTi-like cells in thymus, LNs, and spleen from 4-week-old *E47*$^{-/-}$ or control mouse. (n=3, from three independent experiments) (**H**) Cell number of ILC2 in bone marrow, LNs, and spleen from 4-week-old *E47*$^{-/-}$ or control mouse. (n=3, from three independent experiments) (**I**) PCR analysis involving TCRβ rearrangements in ILC2. Genomic DNAs prepared from thymic ILC2 of *Tcf3*$^{fl/fl}$*Tcf12*$^{fl/fl}$*Il7r*^{Cre} mouse (dKO ILC2), ILC2 from wild-type lung (WT ILC2), CD4 T cells and B cell from WT spleen were analyzed for Dβ2-Jβ2, or Vβ5.1-Dβ2 rearrangements by PCR. Equal DNA quantities were verified by PCR of Thy1 gene. One experiment. (**J**) Cell number of ILC2 in LNs, spleen, and BM from 4-week-old *Tcf3*$^{fl/fl}$*Tcf12*$^{fl/fl}$*Il7r*^{Cre}*Rag2*$^{-/-}$ or *Rag2*$^{-/-}$ mouse. (n=3-6, from three independent experiments) Data represent the mean ± SD. *, $P<0.05$, **, $P<0.01$, ****, $P<0.0001$ (Student's *t* test).

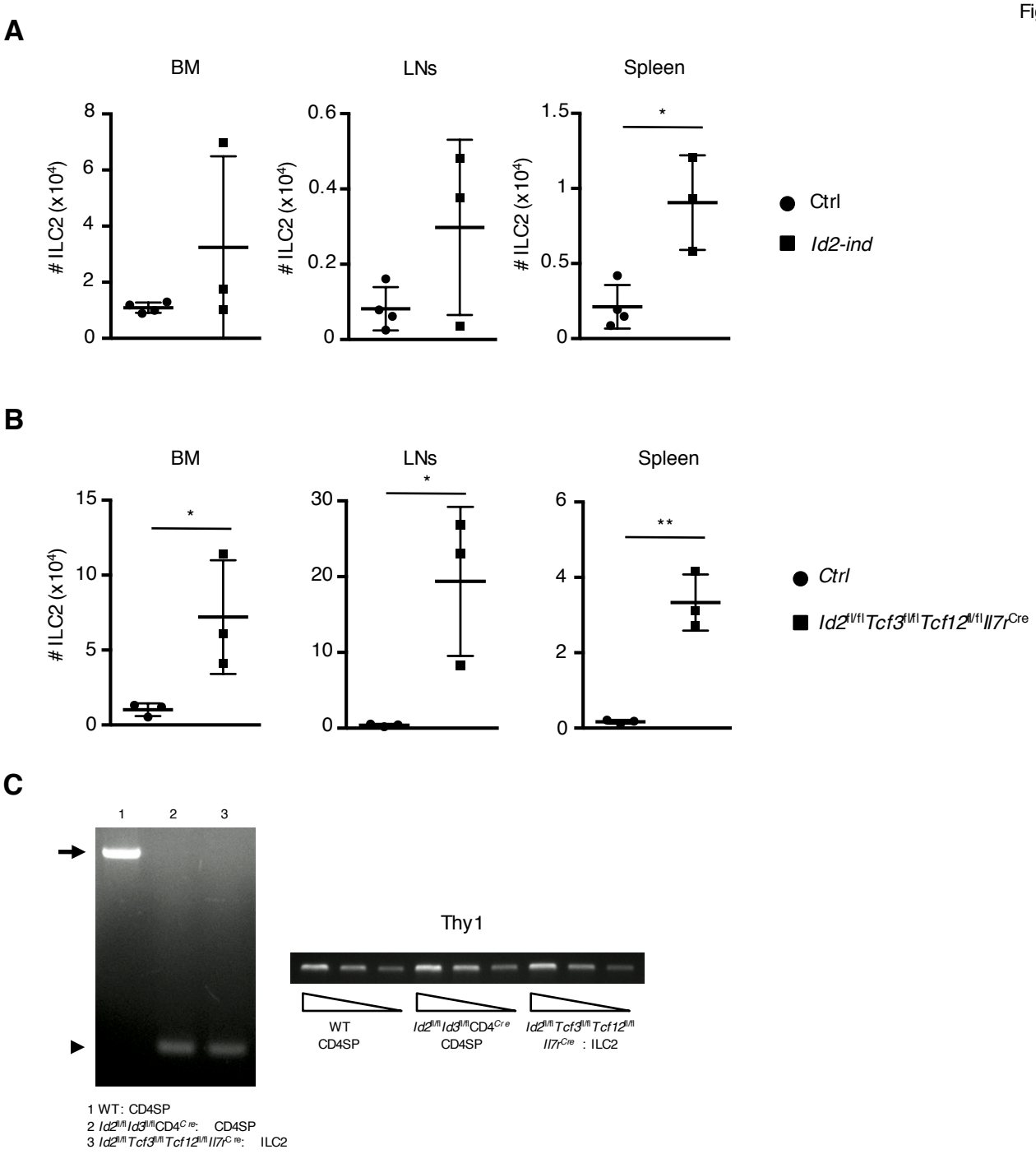

Figure S4 E-Id protein axis control the development of ILCs (Related to Figure 5).
(**A**) Cell number of ILC2 in bone marrow, LNs, and spleen of control and *Id2*-inducible (*Id2*-ind) mice treated with Doxycyclin, as shown in Figure 5. (n=3, one experiment) (**B**) Cell number of ILC2 in bone marrow, LNs, and spleen of 4-week-old control or *Id2*$^{fl/fl}$*Tcf3*$^{fl/fl}$*Tcf12*$^{fl/fl}$*Il7r*^{Cre} mouse. (n=3, from three independent experiments) Data represent the mean ± SD. *, $P < 0.05$, **, $P < 0.01$, ****, $P < 0.0001$ (Student's *t* test). (**C**) PCR analysis for *Id2* gene deletion in thymic ILC2s from *Id2*$^{fl/fl}$*Tcf3*$^{fl/fl}$*Tcf12*$^{fl/fl}$*Il7r*^{Cre} mouse. Genomic DNAs prepared from CD4SP thymocytes from wild-type or *Id2*$^{fl/fl}$*Id3*$^{fl/fl}$*CD4*^{Cre} mouse and thymic ILC2s from *Id2*$^{fl/fl}$*Tcf3*$^{fl/fl}$*Tcf12*$^{fl/fl}$*Il7r*^{Cre} mouse were analyzed for *Id2* gene deletion by PCR. Equal DNA quantities were verified by PCR of Thy1 gene. Arrow indicates wild-type *Id2* gene. Arrowhead indicates deleted *Id2* gene. (One experiment)

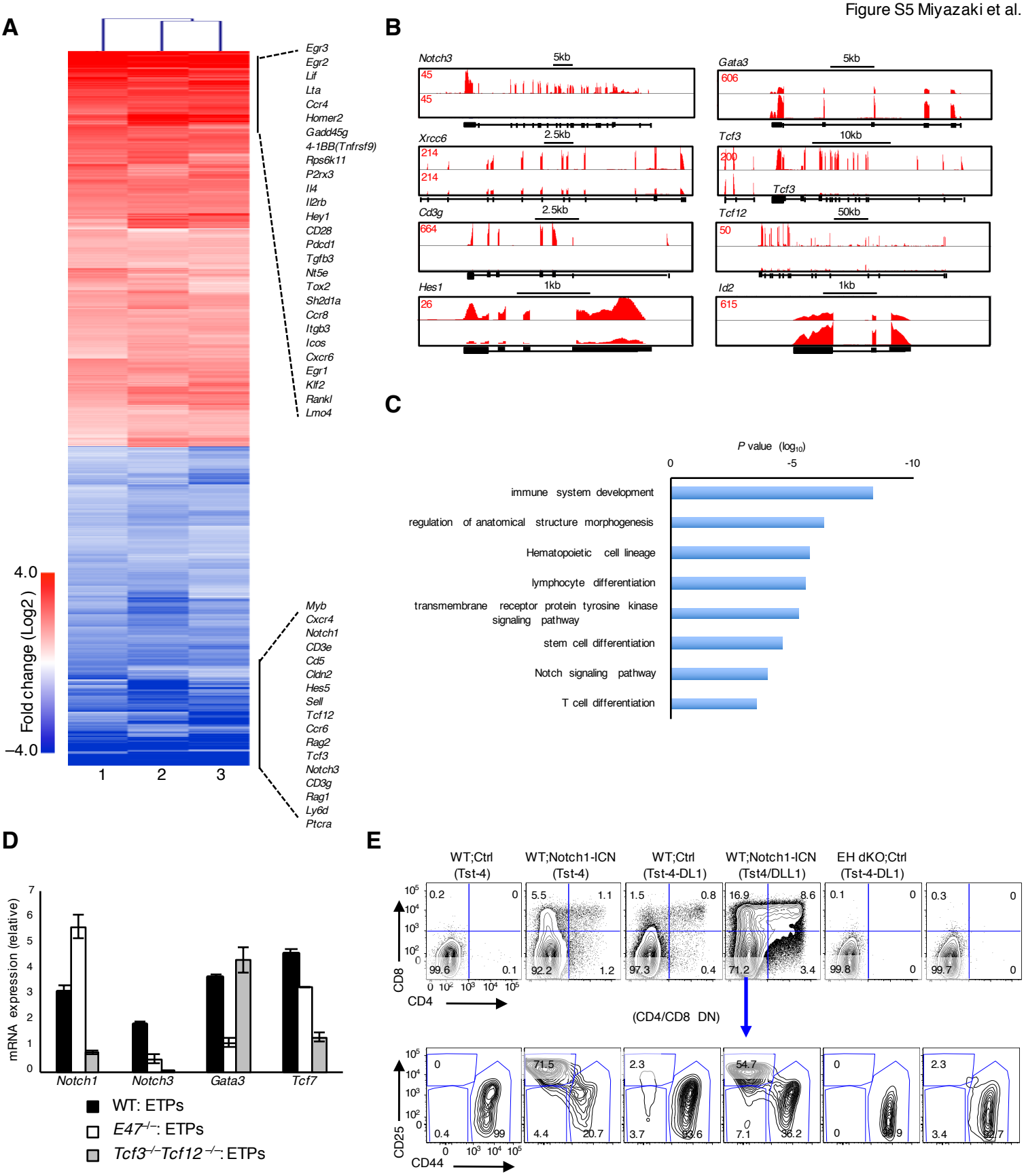

Figure S5 Transcriptome signature of EH dKO ETPs (Related to Figure 6).
(**A**) Heatmap is displayed for significantly differentially expressed genes in ETPs from *Tcf3*$^{fl/fl}$*Tcf12*$^{fl/fl}$*Il7r*^{Cre} fetal thymus, as seen in Figure 7 (> twofold, P <0.05). (**B**) RNA-seq analysis at *Notch3, Xrcc6, Cd3g, Hes1, Gata3, Tcf3, Tcf12*, and *Id2*, presented in reads per million reads aligned (RPM). (**C**) Clusters of genes whose expression was downregulated in *Tcf3*$^{-/-}$*Tcf12*$^{-/-}$ ETPs were identified using GO terms. (**D**) *Notch1, Notch3, Gata3*, and *Tcf7* transcripts in ETPs (CD4^{-}CD8^{-}Lin^{-}CD44^{+}CD25^{-} Kit^{+}) from adult wild-type, *E47*$^{-/-}$, and *Tcf3*$^{fl/fl}$*Tcf12*$^{fl/fl}$*Il7r*^{Cre} mouse, presented relative to the abundance of *Hprt* transcript (encoding hypoxanthine guanine phosphoribosyl transferase). (**E**) Sorted ETPs (CD44^{+}CD25^{-}Kit^{+}) from 14.5 dpc littermate control (WT) or *Tcf3*$^{fl/fl}$*Tcf12*$^{fl/fl}$*Il7r*^{Cre} (EH dKO) fetus were infected with retroviral vectors (pMx) encoding Intracellular murine Notch1 (Notch1-ICN). Then, cells were co-cultured with Tst4 or Tst-4-DL1stroma cells for 10 days. Two independent experiments showed similar results.

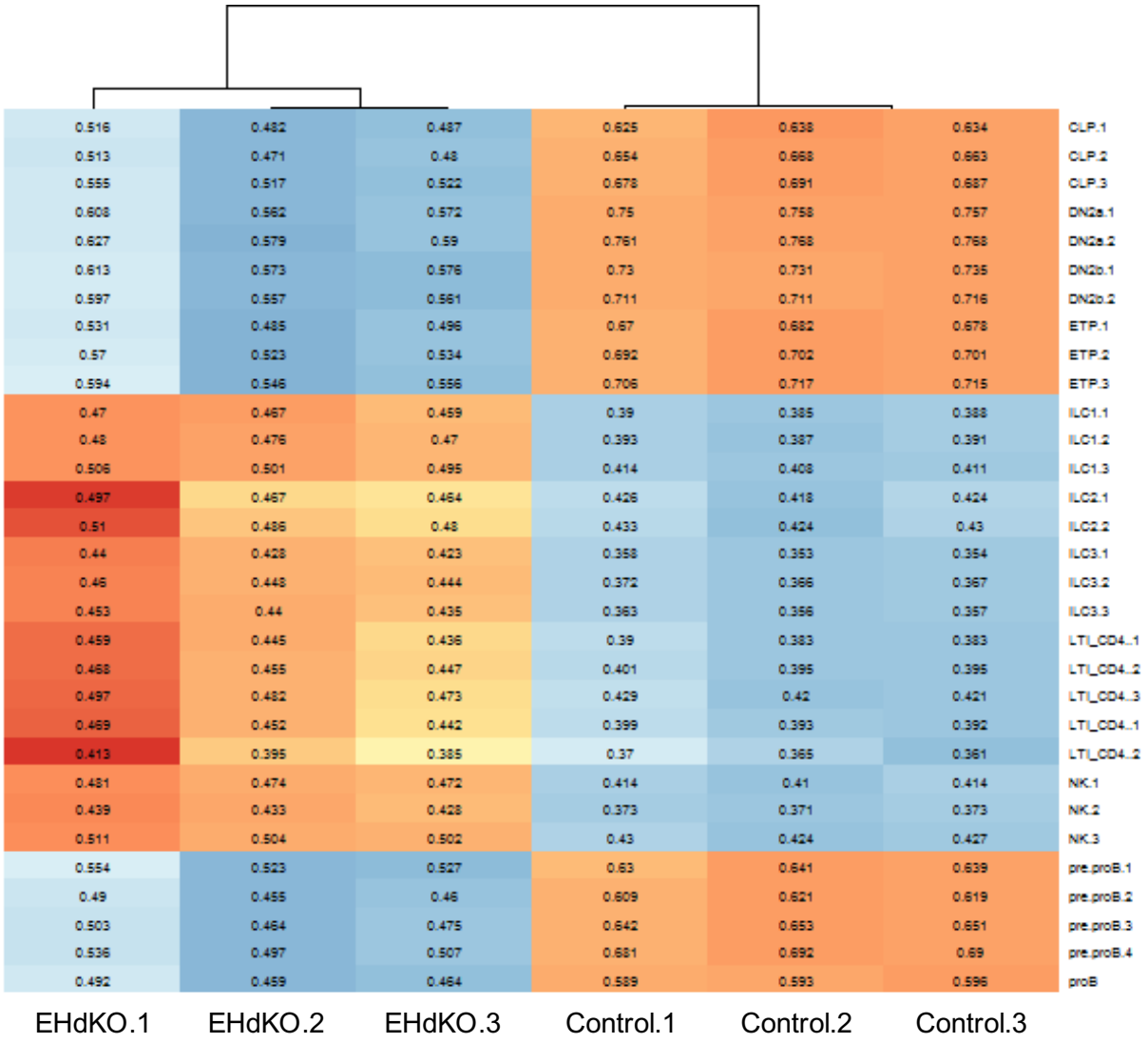

Figure S6 Heatmap of the Spearman's Correlation of the Control and EHdKO RNA-seq data and Immgen Microarray Data of Different Immune Subsets (Related to Figure 6). The gene expression values of the RNA-seq and microarray data were first extracted from a differentially expressed gene list (2710 genes) with a FDR < 0.05 between the Control ETPs and *Tcf3*$^{fl/fl}$*Tcf12*$^{fl/fl}$*Il7r*^{Cre} ETPs (EHdKO). Spearman's correlation were then calculated between the samples, followed by clustering. Three biological replicates of the Control and EHdKO were performed.

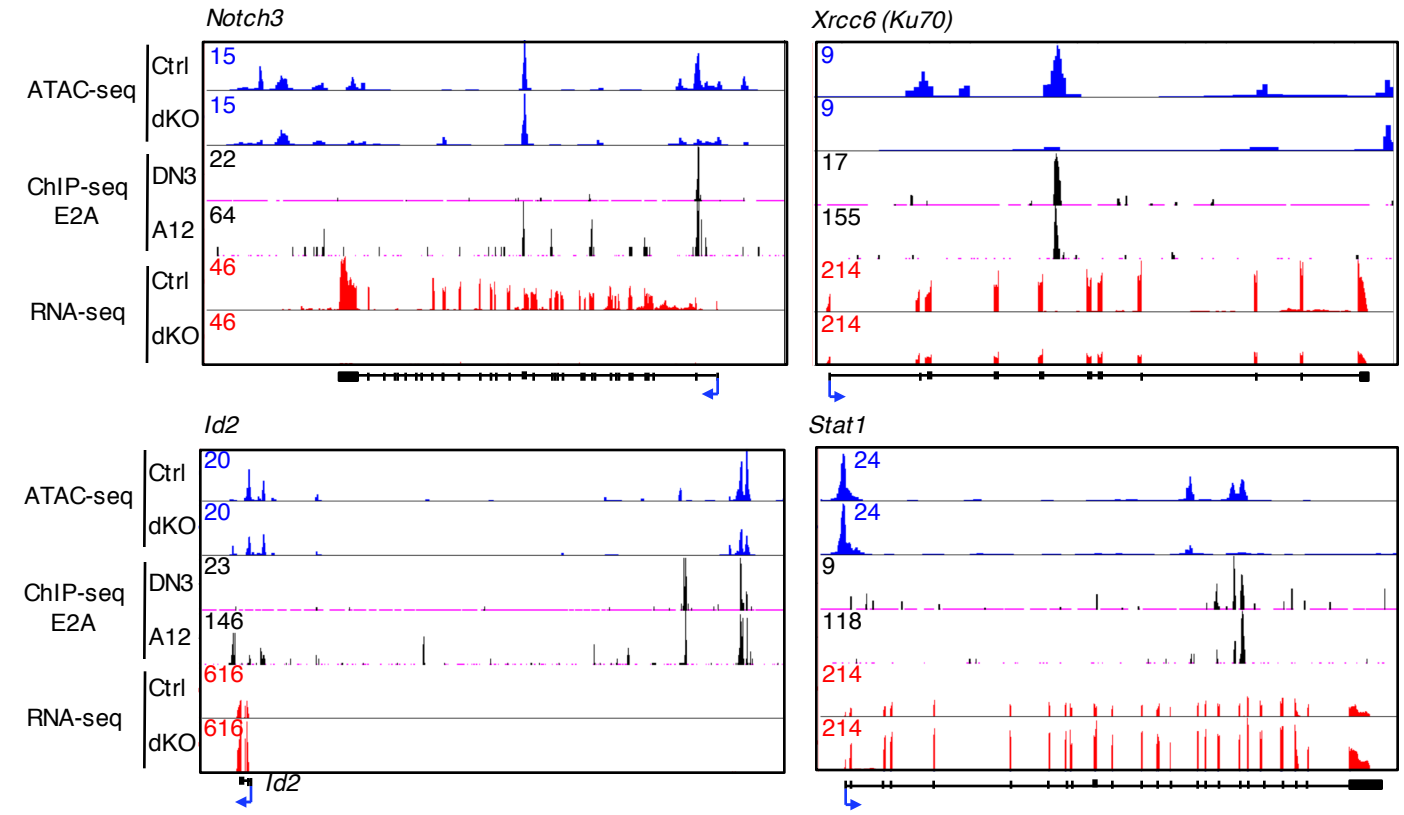

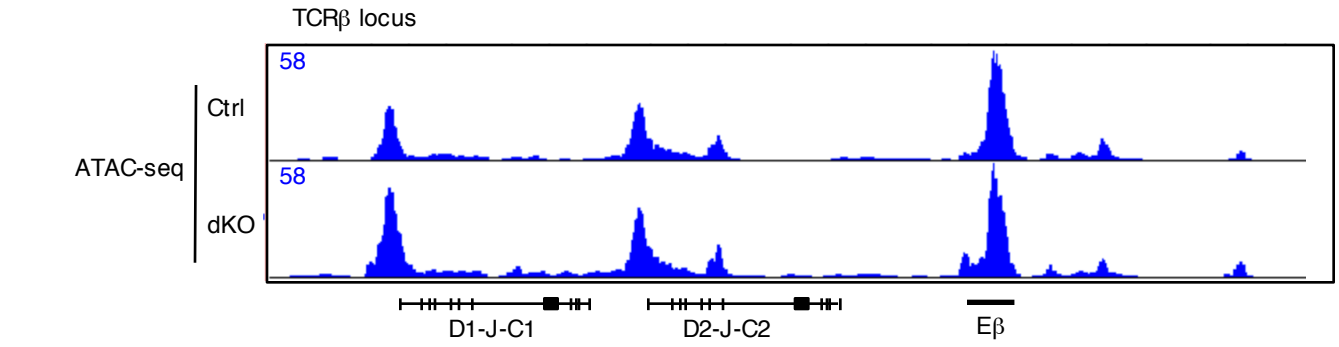

Figure S7 E2A and HEB control a T-lineage specific enhancer repertoire (related to Figure 7).
(**A**) Browser shots of the normalized ATAC-seq and RNA-seq signals at the *Notch3, Xrcc6, Id2*, and *Stat1* loci of the control and *Tcf3*$^{fl/fl}$*Tcf12*$^{fl/fl}$*Il7r*^{Cre} (dKO) ETPs. ChIP-seq, DN3; *Rag2*$^{-/-}$ thymocytes, A12; *E2A*$^{-/-}$ E47-reconstituted T cell line, as seen Figure 7. (**B**) Browser shots of the normalized ATAC-seq signals at the locus of TCRβ D1-J-C1, D2-J-C2, and Eβ of the control and dKO ETPs.

ATAC-Seq mapping summary

Sample name	# Total reads(M)	# Uniquely mapped reads(M)	% Uniquely mapped
EHdKO	225.66	99.45	44.1
EHCont	259.62	99.29	38.3

RNA-Seq mapping summary

Sample name	# Total reads(M)	# Mapped reads(M)	% Mapped
EHCont1	59.54	44.54	74.8
EHCont2	68.59	51.86	75.6
EHCont3	71.65	54.80	76.5
EHdKO1	82.08	63.78	77.7
EHdKO2	78.57	59.87	76.2
EHdKO3	74.83	57.70	77.1

Table S1 (Related to Figure 7). Summary of reads obtained from RNA-seq and ATAC-seq analysis for ETPs from *Tcf3*$^{fl/fl}$*Tcf12*$^{fl/fl}$*Il7r*^{Cre} (EHdKO) and littermate control (EHCont) fetal thymi.